ACI STRUCTURAL JOURNAL TECHNICAL PAPER

Title No. 116-S90

Cyclic Crack-Slip Model for Smeared Rotating Crack Formulations

by Anca C. Ferche and Frank J. Vecchio

An analytical model describing crack-slip behavior, compatible with smeared crack models and suited for the finite element analysis of reinforced concrete specimens subjected to reversed cyclic loading conditions, is presented. The procedure, largely based on Walraven's monotonic formulation, calculates slip as a function of the shear stress along the crack surface, accounting for cyclic degradation due to load reversals. The formulation is compatible with a smeared rotating-crack approach in finite element analysis procedures, and has been implemented within the algorithms of VecTor2, an in-house two-dimensional nonlinear finite element program. The model keeps track of two distinct independent cracks within one element by monitoring the change in direction of the principal stress field. A cyclic degradation law is empirically derived from tests performed on push-off specimens. Herein, verification studies undertaken on concrete shell elements and shear walls are presented, indicating the suitability of the approach for modeling the reversed cyclic response of reinforced concrete. Accounting for slip results in more accurate estimates of deformation response, energy dissipation, and failure mode.

Keywords: crack slip; cyclic loading; reinforced concrete; shear capacity; strength degradation.

INTRODUCTION

The behavior of reinforced concrete (RC) elements subjected to reversed cyclic loading conditions has attracted considerable experimental and analytical research interest,[1-13] particularly as force-based seismic design methods have gradually been replaced by displacement-based methods. The accurate assessment of strength, ductility, and energy dissipation of components has become of paramount significance in design and structural appraisal. Earthquakes subject structures to repeated load reversals, which may induce strength and stiffness degradation in the structure's response and cause premature failure. Advanced modeling techniques are often employed to assist rehabilitation, structural reassessment, and design. However, modeling reinforced concrete components subjected to reversed cyclic loading is still a challenging task, particularly due to the complex mechanisms that influence the response.

The nonlinear finite element analysis program VecTor2,[14] developed at the University of Toronto, has proven to be a viable tool for the analysis of two-dimensional reinforced concrete structures subjected to complex types of loading.[10,12,15,16] The Disturbed Stress Field Model[17] (DSFM) forms the theoretical basis of the program. The DSFM, a smeared crack model, is a hybrid formulation between a fully rotating crack model and a fixed crack model. Based on the Modified Compression Field Theory[18] (MCFT), the DSFM considers equilibrium, compatibility, and constitutive relationships in terms of average stresses and strains measured over the gauge length of a few cracks. The main advancement beyond the MCFT is the inclusions of compatibility relationships which incorporate the slip along crack surfaces.

For a finite element analysis to capture the response of a reinforced concrete structure subjected to cyclic or reversed cyclic loading, several mechanisms need to be considered: concrete strength enhancement due to confinement, tension softening, tension stiffening, reinforcement buckling, bond slip, hysteretic behavior for concrete and reinforcement, and slip along crack interfaces. Depending on characteristics such as loading protocol, specimen design, and boundary conditions, some of these mechanisms may have a more notable influence on the response than others.

A reinforced concrete element subjected to inelastic cyclic loading develops cracks that, depending on the load direction, open and close, transferring shear stresses across their surfaces, and eventually developing slip. The crack-slip mechanism is an important energy dissipation source that was found[19,20] to have a pronounced effect for structures subjected to high shear demand, and for lightly reinforced structures, due to the load transfer mechanism. Both instances are associated with brittle and sudden failures.

Tests conducted on RC membrane and shell elements[21-25] suggest that reserved cyclic shear demand tends to cause strength and stiffness degradation in the response compared to monotonic shear. Although the tests performed are not exhaustive in the context of parameters investigated, the general trend is that the cyclic degradation is proportional to the shear stress applied. Cycles performed at a lower shear stress demand, prior to yielding of the reinforcement, did not produce a significant increase in damage. However, after yielding of the reinforcement, repeated loading at the same level of shear stress produced higher shear stains with each cycle, ultimately causing failure. In this work, the deterioration in response is investigated through the damage induced at the crack interfaces, which is addressed through the crack-slip model.

A significant amount of experimental research was conducted in the past few decades on crack-slip behavior,[26-31]

ACI Structural Journal, V. 116, No. 4, July 2019.

MS No. S-2018-274, doi: 10.14359/51715564, was received July 18, 2018, and reviewed under Institute publication policies. Copyright © 2019, American Concrete Institute. All rights reserved, including the making of copies unless permission is obtained from the copyright proprietors. Pertinent discussion including author's closure, if any, will be published ten months from this journal's date if the discussion is received within four months of the paper's print publication.

the majority of which was performed using push-off tests. Three main types of specimens can be distinguished based on the crack interfaces: uncracked, pre-cracked, and cold-joint interfaces. In addition, different approaches were taken regarding the reinforcement: embedded in the specimens, debonded, or applied externally to act as restraint. Constant and variable crack widths were investigated, and the loading protocol was either monotonic, cyclic, or reversed cyclic. The tests revealed several characteristics of the crack-slip behavior: initially constant stiffness during the first cycle that eventually decreases as the stress increases; significant residual slip after the load is removed; a period of low initial stiffness in the subsequent cycles is followed by stiffening with increasing slip; decrease in stiffness with crack width increase; and load amplitude influence on the slip developed.

Numerous empirical formulations of different complexities on crack-slip behavior were developed. Walraven[32] proposed a monotonic relationship for the slip along the crack as a function of the shear stress on the crack, the width of the crack, and the concrete strength, compatible with smeared rotating crack formulations and adopted by the DSFM. Tassios and Vintzeleou[30] developed a crack-slip model for both rough and smooth interfaces, which included a cyclic degradation law for the shear stress across the crack and the width of the crack based on the number of cycles experienced for a given slip. Another notable contribution was the contact density model developed by Li et al.,[31] which accounted for the shear, as well as the compressive stress at the crack interfaces, and it was verified against monotonic, cyclic, and reversed cyclic loading on the crack. The model did not include a cyclic degradation law. Bažant and Gambarova[33] developed a monotonic empirical model for crack behavior relating shear stresses to normal stresses to slip displacements along the crack. Dabbagh and Foster[34] developed a monotonic crack-slip model based on the experimental work carried out by Walraven,[32] suited for smeared fixed-crack formulations that performed well for the analysis of shear-critical beams. Calvi et al.[20] proposed a comprehensive model for the crack-slip behavior suited for monotonic, cyclic, and reversed cyclic loading on the crack interfaces. The empirical parameters of the model were calibrated based on tests performed on pre-cracked reinforced concrete panels.

The crack-slip model proposed in this paper attempts to increase the suitability of smeared rotating crack models for the analysis of structures under cyclic and reversed cyclic loadings. It incorporates an empirical cyclic degradation law, and it employs two independent cracks within one finite element. The model captures the observed crack-slip behavior performed on push-off tests and has proven to perform well within the smeared crack formulation of the DSFM.

RESEARCH SIGNIFICANCE

Most smeared rotating crack models, such as the DSFM, employ certain assumptions in their formulation which may make them potentially unconservative for cyclic mechanisms. The crack-slip model presented herein addresses these assumptions, and its implementation within smeared crack formulations increases their suitability for the analysis of RC elements subjected to cyclic and reversed cyclic loading conditions.

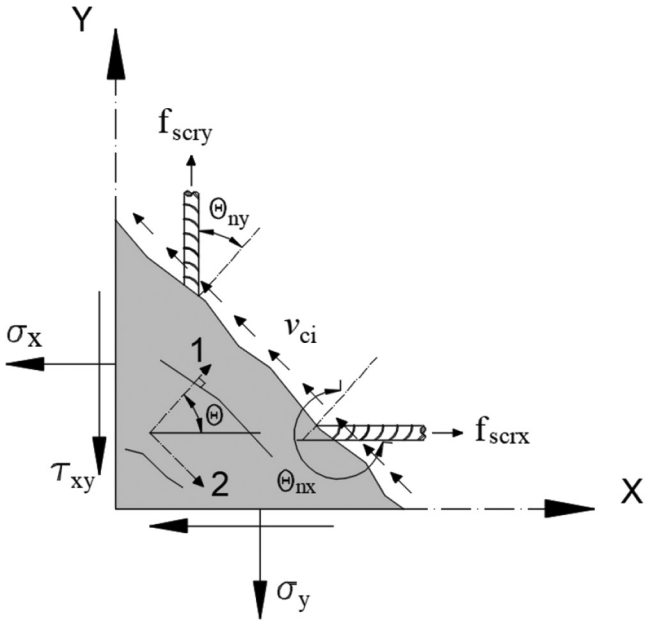

Fig. 1—Local crack conditions.

CRACK-SLIP MODEL

For one rectangular concrete finite element (FE) with orthogonal reinforcement and subjected to reversed cyclic shear, the DSFM formulation calculates crack rotations in the range of 90 degrees as the load changes direction. The slip along the crack developed during positive loading fully recovers as the load is reversed, without plastic deformations. This crack behavior is somewhat unsatisfactory and not consistent with experimental observations of residual slip deformations upon load removal. The proposed methodology addresses this issue with two independent alternately active cracks, depending on load direction. The slip strains developed in the positive and negative cycles are treated independently during the analysis. This strategy permits the implementation of a crack-slip degradation model appropriate for RC under reversed cyclic loading.

Previous crack-slip model

The DSFM solution procedure uses an incremental total-load, iterative, secant stiffness formulation. The original crack-slip model used within the DSFM evaluates the slip along the crack δ_s (mm), as a function of the shear stress on the crack surface v_{ci} (MPa), shear resistance due to dowel action v_d (MPa), average crack width w (mm), and concrete cube strength f_{cc} (MPa)

$$\delta_s = \frac{|v_{ci}| - v_d}{1.8w^{-0.8} + \left(0.234w^{-0.707} - 0.20\right)\cdot f_{cc}} \quad (1)$$

Shown in Fig. 1 are the local crack conditions for the particular case of orthogonal reinforcement. The shear stress on the crack surface v_{ci} is evaluated from equilibrium conditions as

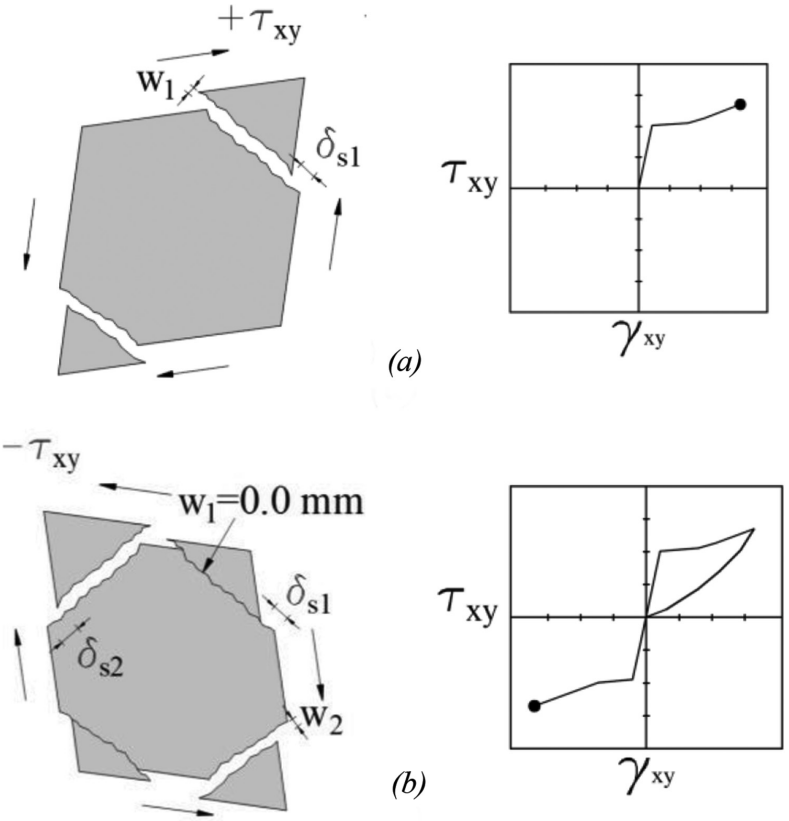

Fig. 2—Total deformations: (a) first positive shear cycle; and (b) negative shear cycle.

$$v_{ci} = \sum_{i=1}^{n} \rho_i \left(f_{scri} - f_{si} \right) \cdot \cos\theta_{ni} \cdot \sin\theta_{ni} \quad (2)$$

where ρ_i is reinforcement ratio; f_{scri} is local reinforcement stress at the crack; f_{si} is average reinforcement stress; and angle θ_{ni} is the difference between the angle of orientation of the reinforcement and the normal to the crack surface.

The shear resistance due to dowel action v_d is evaluated based on the model proposed by He and Kwan,[35] detailed in Wong et al.,[14] and expressed as a function of the slip along the crack δ_s.

The average crack width w is calculated as the product of the average tensile strain ε_1 and the average crack spacing s, as

$$w = \varepsilon_1 \cdot s \quad (3)$$

The crack spacing s may be determined from field measurements; or alternatively, it is calculated as a function of the orientation of the stress field θ and the crack spacing parameters with respect to the x- and y-directions, s_x and s_y, using the CEB-FIP 1978[36] model for deformed bars. The parameter s_x is the average crack spacing that would result from longitudinal tension, and s_y is the average crack spacing that would result from transverse tension

$$s = \frac{1}{\frac{\sin\theta}{s_x} + \frac{\cos\theta}{s_y}} \quad (4)$$

Two independent cracks

To model the observed cyclic crack behavior in the context of a smeared rotating crack formulation, two different crack directions have to be considered (Fig. 2). The two independent and alternately active cracks undergo cyclic shear as the applied load changes direction. The deformations due to slip along the crack, δ_{s1}, experienced during the positive loading phase (Fig. 2(a)), are treated as plastic unrecoverable deformations as the load is reversed, and the second crack is activated (Fig. 2(b)).

Each of the two cracks is allowed to rotate 30 degrees relative to their initial direction. The rotation limit was set based on experimental observations[37] which suggest a maximum change in the orientation of the principal stress field of 30 degrees for monotonic loading conditions. The second crack is activated when the direction of the first crack changes with more than 70 degrees from its initial orientation.

Cyclic degradation law

Two key features were considered for the experiments selected for the development of the crack-slip degradation law: cyclic loading on the crack interfaces, and a reasonably high number of cycles. Although cyclic tests on crack interfaces are not numerous enough to develop a statistically strong model, they are representative for the crack behavior of a RC element subjected to reversed cyclic shear. The cyclic tests performed by Paulay and Loeber[26] and Briseghella and Gori[27] on push-off tests were chosen to define the crack-slip degradation law. Shown in Fig. 3 are typical responses obtained during the tests. The cyclic damage on the crack

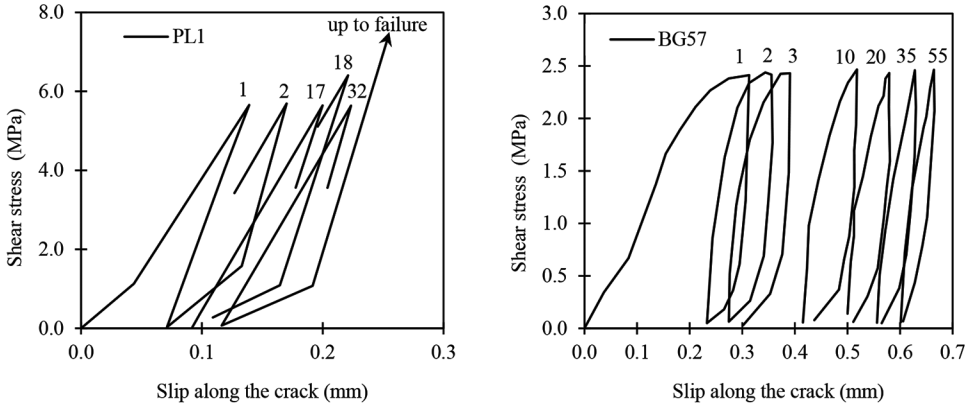

Fig. 3—Crack-slip response: (a) Paulay and Loeber[26]; and (b) Briseghella and Gori.[27] (Note: 1 MPa = 0.145 ksi; 1 mm = 0.0394 in.)

interfaces was expressed through a degradation factor as the ratio between the slip measured during the first cycle and the slip measured in the subsequent cycles for the same shear stress on the crack. Figure 4 shows a compilation of the degradation factors calculated from the tests versus the number of cycles. The degradation law expresses the degradation factor *DF* with respect to the number of loading-unloading cycles *N* experienced by the crack, as such

$$DF = \begin{cases} 0.9994 \cdot N^{-0.154} & \text{for } N \le 60 \\ 0.531 & \text{for } N > 60 \end{cases} \quad (5)$$

The maximum number of cycles performed during the selected cyclic tests was 60; therefore, with the lack of experimental data, a cap-off was applied for more than 60 cycles in terms of the degradation factor. The degradation law does not consider directly for the level of shear stress across the crack; however, it is indirectly factored in through the slip, which is a function of the shear stress. Other researchers[30] have successfully addressed cyclic degradation through relationships dependent on the number of cycles.

Shown in Fig. 5 is the behavior of the system of two cracks as one RC rectangular finite element is experiencing reversed cyclic shear loading. The analysis is performed in load-controlled conditions, with 6.2 MPa peak shear stress applied each cycle. The stress amplitude was chosen such that it would bring the transverse reinforcement to the onset of yielding as based on experimental observations; degradation in response was observed to be significant only upon yielding of the reinforcement. The concrete compressive strength is 37 MPa, and the reinforcement ratios are 3.0% in the x-direction, and 1.0% in the y-direction. For this particular case, positive shear loading causes positive slip and crack shear stress, while negative shear causes negative slip and crack shear stress. Note that the opposite phenomenon occurs if the reinforcement ratio in the x-direction is smaller than in the y-direction.

Figures 5(a), 5(b), and 5(c) show the first positive cycle, during which only one crack is active. The loading phase is composed of branches 0-A-B-C, while C-D represents the unloading phase (Fig. 5(a) and 5(b)). The slip is calculated using Eq. (1) for branches 0-A, and B-C. When the

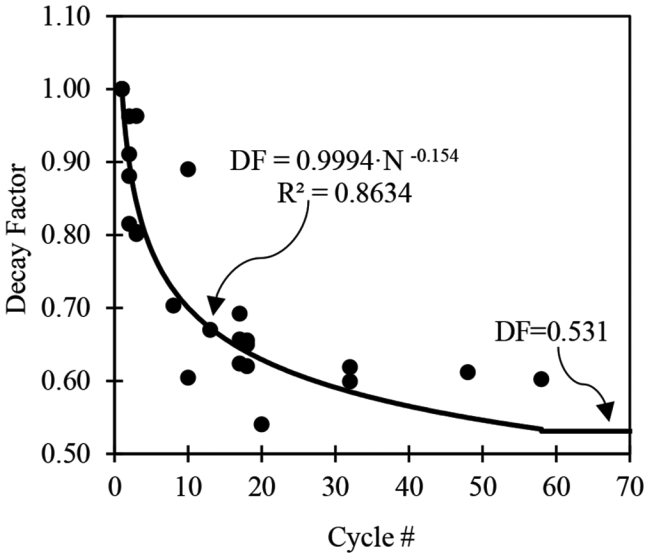

Fig. 4—Decay factor versus number of cycles.

shear stress on the crack reduces as a result of crack rotation (A-B), or when the load is reversed (C-D), the slip along the crack is calculated based on Eq. (6), not allowing for slip recovery

$$\delta_{s1} = \max(\delta_s, \delta_{s.i-1}) \quad (6)$$

where δ_s is evaluated based on Eq. (1); and $\delta_{s.i-1}$ is the slip along the crack calculated in the previous load stage.

During the first negative cycle (Fig. 5(d)), the first crack direction remains inactive (Fig. 5(e)) while the second crack direction is activated (Fig. 5(f)). The second crack behavior is treated identically as the first crack, taking into account that the shear stress on the crack and the slip are negative.

Subsequent cycles involve monitoring the number of load reversals and employing in the slip calculation the cyclic degradation factor defined by Eq. (5). Shown in Fig. 5(g), 5(h), and 5(i) are the total shear stress versus total shear strain, first crack behavior, and second crack behavior during three complete reversed loading cycles. Reloading in positive shear reactivates the first crack (Fig. 5(h)). Similar behavioral relationships are assumed for both crack directions as they take turn being active.

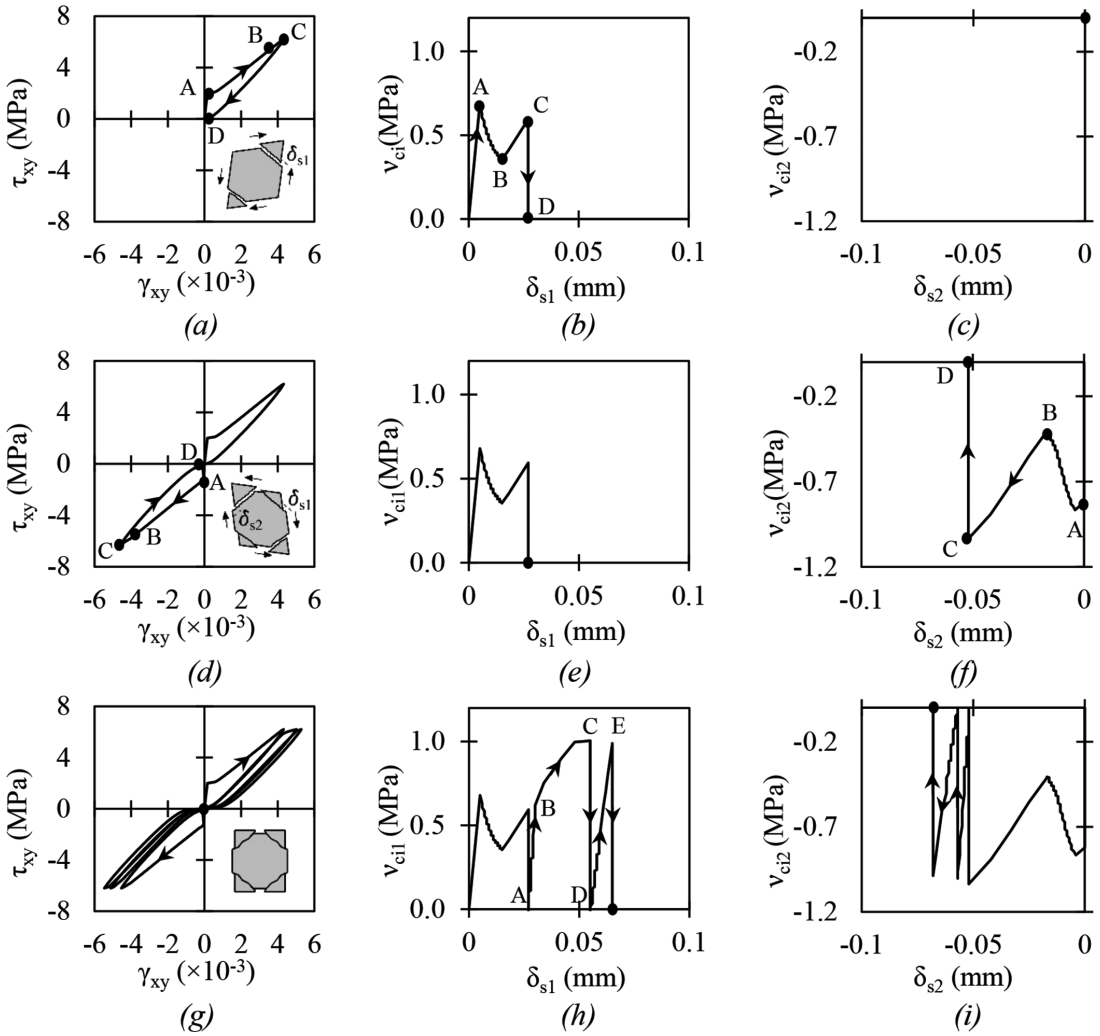

Fig. 5—Slip along crack, δ_{s1} and δ_s, versus shear stress along crack, v_{ci1} and v_{ci2}, presented alongside total shear stress τ_{xy} and total shear strain γ_{xy}. (Note: 1 MPa = 0.145 ksi; 1 mm = 0.0394 in.)

To highlight the reloading slip calculation, Fig. 6 shows the first reloading excursion for the first crack.

The crack stiffness G_{s1} is defined as

$$G_{s1} = \frac{v_{ci1.\max}}{\delta_{s1.\max} \cdot \left(\frac{1}{DF_1} - 1\right)} \tag{7}$$

where $v_{ci1.\max}$ is the maximum shear stress on the crack developed before unloading in the previous cycle; $\delta_{s1.\max}$ is the corresponding slip; and DF_1 is the degradation factor for the first crack evaluated based on Eq. (5).

The slip on the reloading branch, when the shear stress on the crack v_{ci1} is smaller than $v_{ci1.\max}$, is evaluated using

$$\delta_{s1} = \max\left(\delta_{s1.\max} + \frac{v_{ci1}}{G_{s1}}, \delta_{s.i-1}\right) \tag{8}$$

When v_{ci1} exceeds $v_{ci1.\max}$, the slip is calculated as

$$\delta_{s1} = \max(\delta_s, \delta_{s.i-1}) \tag{9}$$

The unloading phase is identical to the unloading during the first cycle. A similar approach is used for calculating the behavior of the second crack, accounting for the negative values of the slip and shear on the crack.

Slip strain vectors

The procedure of translating the discrete crack slip into element strains is described by Vecchio.[17] The effective slip shear strain is defined as the ratio between the slip δ_{si} (mm) and the crack spacing s (mm)

$$\gamma_{si} = \frac{\delta_{si}}{s},\ i = 1,2 \tag{10}$$

The components of the slip strain vectors for both crack directions, $[\varepsilon^{s1}]$ and $[\varepsilon^{s2}]$, are determined using Mohr's circle; as such

$$\varepsilon_x^{si} = \frac{\gamma_{si}}{2} \cdot \sin 2\theta,\ i = 1,2 \tag{11}$$

$$\varepsilon_y^{si} = \frac{\gamma_{si}}{2} \cdot \sin 2\theta,\ i = 1,2 \tag{12}$$

$$\gamma_{xy}^{si} = \gamma_{si} \cdot \cos 2\theta,\ i = 1,2 \tag{13}$$

where θ is the orientation of the principal stress field.

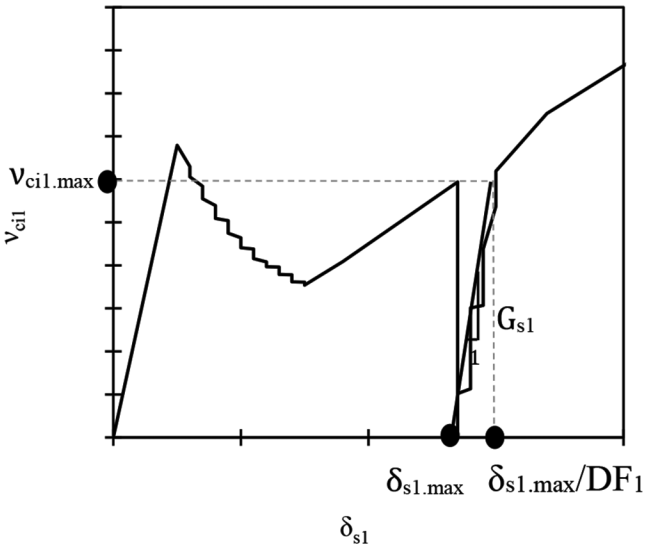

Fig. 6—Shear stress on crack versus slip along crack during reloading.

The total strains [ε] at a point in a reinforced concrete continuum represent the summation of: the net concrete stress-induced strains [ε_c]; the elastic concrete strain offsets [ε_c^o] due to mechanisms such as thermal expansion, prestrains, shrinkage, and lateral expansion; the plastic concrete strain offsets [ε_c^p] due to cyclic loading or damage effects; and the strains due to shear slip along the crack [ε^{s1}] and [ε^{s2}]. Consequently, the compatibility relationship for concrete in two-dimensions is

$$[\varepsilon] = [\varepsilon_c] + [\varepsilon_c^o] + [\varepsilon_c^p] + [\varepsilon^{s1}] + [\varepsilon^{s2}] \quad (14)$$

$$\left[\varepsilon^{s1}\right] = \begin{bmatrix} \varepsilon_x^{s1} \\ \varepsilon_y^{s1} \\ \gamma_{xy}^{s1} \end{bmatrix}; \left[\varepsilon^{s2}\right] = \begin{bmatrix} \varepsilon_x^{s2} \\ \varepsilon_y^{s2} \\ \gamma_{xy}^{s2} \end{bmatrix} \quad (15)$$

VERIFICATION STUDIES

Verification studies were undertaken to obtain an indication of the stability and accuracy of the procedure when applied to the analysis of reinforced concrete elements subjected to cyclic loading. The results obtained from the analyses of concrete shell elements and shear walls are presented. Table 1 summarizes the properties of the specimens.

Analysis of concrete shell elements

Concrete shell elements subjected to reversed cyclic shear loading, tested by Stevens[21] and Ruggiero[25] were analyzed. One rectangular finite element was used to represent the shell elements, given the uniform material properties and stress conditions. The analyses were performed in load-controlled conditions, replicating the experimental loading history. Although VecTor2[14] provides an extended selection of behavioral models for each mechanism, the default options were used in the analyses, with the exception of the crack-slip model.

Figure 7 summarizes the measured versus calculated responses for all the shell elements. Two analysis results are presented for each specimen: the first using the original crack-slip formulation, without slip degradation (labeled "w/o slip deg.") and the second using the proposed model (labeled "w slip deg."). Note that the analyses performed neglecting the slip degradation due to cyclic loading in the analysis do not calculate failure of the elements through cycling at the ultimate shear stress level during the tests, regardless of the number of cycles applied. The hysteresis loops stabilize, and are identical for each cycle performed at the same shear stress. Using the proposed methodology, upon yielding of the transverse reinforcement, the calculated strains increase as a consequence of cycling at the same stress level; finally, the specimens fail in shear. The analytical behavior is consistent with the experimental observations. Although the hysteresis loops are not replicated perfectly, the proposed crack-slip model performs reasonably well, confirming an important experimental concept: failure of a concrete element can be reached analytically by cycling at the same level of stress.

Analysis of shear walls

To further test the validity of the proposed model, cantilever shear walls subjected to reversed cyclic conditions were analyzed: Wall B2 tested by the Portland Cement Associaion[1] (PCA), Wall RW1 tested by Thomson and Wallace,[4] and Walls LSW1 and LSW2 tested by Salonikios et al.[6] The specimens are part of series of walls extensively used for validation studies. The loading protocol, together with the yielding of reinforcement in the early cycles, make these specimens good candidates for verifying the proposed procedure. With aspect ratios larger than 2.0, Specimens B2 and RW1 are classified as slender walls, while Specimens LSW1 and LSW2, with aspect ratios equal to 1.0, may be considered squat shear walls. Different reinforcement ratios were provided for the webs of the walls and their boundaries, as shown in Table 1.

The B2 wall was barbell-shaped, with a total width of 1910 mm (75 in.), and a height of 4570 mm (180 in.). The boundary elements were 305 mm (12 in.) square, and the web was 102 mm (4 in.) thick. Stiff top and bottom beams were monolithically built with the wall. The reversed cyclic loading protocol consisted of three lateral imposed displacements, progressively increasing in amplitude. No axial loading was applied.

The FE model (Fig. 8(a)) consisted of 1160 rectangular elements with the reinforcement represented as smeared within the concrete elements. The base of the wall was considered fully fixed. Loading was imposed at the center node in the middle of the top beam.

Rectangular wall RW1 was 1220 mm (48 in.) wide, 3658 mm (144 in.) tall, and with a thickness of 102 mm (4 in.). Stiff top and bottom boundary elements were provided for load transfer and anchorage to the strong floor. Progressively increasing reversed cyclic lateral displacements were applied at the top of the specimen. An axial load equal to $0.10A_gf_c$ (where Ag is the wall's cross-sectional area) was maintained constant throughout the test at the top of the wall. The FE model, made up of 2669 rectangular elements is shown in Fig. 8(b). Similarly to the FE model for Wall B2, the reinforcement was represented as smeared, the base was fully fixed, and the lateral loading was imposed

Table 1—Specimen properties

Test unit	f_c^*, MPa	ρ_x, % ρ_y, % ρ_z, %	f_{yx}, MPa f_{yy}, MPa f_{yz}, MPa
Ruggiero,[25] concrete shells			
SR5	49.5	2.86 0.451 —	411 492 —
SR6	45.4	2.90 0.458 0.307	453 492 474
SR7	32.6	2.85 0.675 —	453 492 —
SR8	33.9	2.87 0.679 0.545	453 492 474
SR9	29.4	2.87 0.679 0.852	453 492 474
Stevens,[21] concrete shell			
SE8	37.0	3.00 1.00 —	492 479 —
Osterele et al.,[1] shear wall			
		web / b.e.†	web / b.e.†
B2	53.6	0.63 / 0.28 0.29 / 3.67 — / 0.125	533 / 533 533 / 410 — / 533
Thomsen and Wallace,[4] shear wall			
		web / b.†	web / b.†
RW1	31.6	0.329 / 1.28 0.329 / 2.92 — / 0.49	413 / 413 413 / 431 — / 413
Salonikios et al.,[6] shear walls			
		web / b.‡	web / b.‡
LSW1	22.2	0.565 / 1.43 0.565 / 1.70 — / 0.50	610 / 610 610 / 585 — / 610
LSW2	21.6	0.277 / 1.43 0.277 / 1.30 — / 0.50	610 / 610 610 / 585 — / 610

*Concrete compressive strength at test day.

†Boundary elements reinforcement.

‡Boundary reinforcement

Note: 1 MPa = 0.145 ksi.

at the middepth of the top beam, allowing rotation. The axial load of 392 kN (88.13 kip) was distributed along the top boundary element, maintained constant during the analysis.

The LSW1 wall had a height and width of 1200 mm (47.2 in.), and a thickness of 100 mm (3.9 in.). It had a rectangular cross section and stiff top and bottom beams cast with the wall. The reversed cyclic loading was applied to the top beam, starting at 2.0 mm (0.079 in.) imposed displacement, with three repetitions, and a cyclic increment of 2.0 mm (0.079 in.) until failure. No axial load was applied. The FE model consisted of 1195 rectangular elements and is shown in Fig. 8(c). The difference between Walls LSW2 and LSW1 consisted of the reinforcement ratios provided, as shown in Table 1.

A summary of the results of the analytical study is shown in Fig. 9 for all shear wall specimens. Wall B2 failed due to crushing of the concrete in the web, reaching a maximum load of 680 kN (152.8 kip), at an ultimate top displacement of 127 mm (5 in.). Figure 9(a) shows the comparison for Wall B2 between the experimental and analytical responses obtained without considering slip degradation. The computed response results in a maximum load of 787 kN (176.9 kip) at an ultimate displacement of 204 mm (8.03 in.), thus overestimating the load capacity by 15% and the ultimate displacement by 60%. In the same fashion, Fig. 9(b) shows the analytical results obtained with the proposed crack-slip model, considering slip degradation. Better estimates were obtained with the peak load of 672 kN (151 kip) and the ultimate displacement of 120 mm (4.72 in.), the analytical results nearly matching the experimental ones perfectly. The degree of pinching of the hysteresis loops was also captured relatively well. Both analysis, with and without slip degradation, captured correct the failure mode.

The results obtained for Wall RW1 are presented in a similar manner in Fig. 9(c) and 9(d). For this wall, failure occurred due to extensive crushing of the boundary elements. A peak load of 148 kN (33.27 kip) was measured and an ultimate displacement of 77 mm (3 in.). The results obtained with the crack-slip model with slip degradation (Fig. 9(d)) again show better agreement with the experimental response compared with the results obtained without slip degradation (Fig. 9(c)). The analysis with the proposed model yielded 158 kN (35.52 kip) peak load and 90 mm (3.54 in.) ultimate displacement, while the results without slip degradation were 161 kN (36.2 kip) for the peak load and 99 mm (3.9 in.) ultimate displacement. The difference in the calculated response is not as significant as for Wall B2. This is due to the effect of the axial loading applied to Specimen RW1. Compression stresses tend to reduce the width of the cracks that form due to lateral displacement and, in turn, the slip is diminished. Analytically, the crack-slip mechanism has a less pronounced effect, compared with specimens experiencing larger crack widths.

Figures 9(e) and 9(f) show the results for squat shear wall LSW1, while Fig. 9(g) and 9(h) do so for LSW2. Similar trends are observed in both cases: the analyses performed with slip degradation calculated somewhat lower maximum loads compared to the analyses without slip degradation. For wall specimen LSW1, the model without slip degradation yielded a maximum load of 281 kN and an ultimate displacement of 11 mm compared to 271 kN and 9.2 mm for the analysis with slip degradation. Wall specimen LSW2 has a calculated peak load of 208 kN and an ultimate displacement of 12.25 mm without slip degradation, and 205 kN maximum load and 9.8 mm ultimate displacement with slip degradation. There is a good agreement in terms of stiffness, ductility, peak load, degree of pinching of the hysteresis loops, and dissipated energy, better than that obtained when crack-slip degradation is neglected.

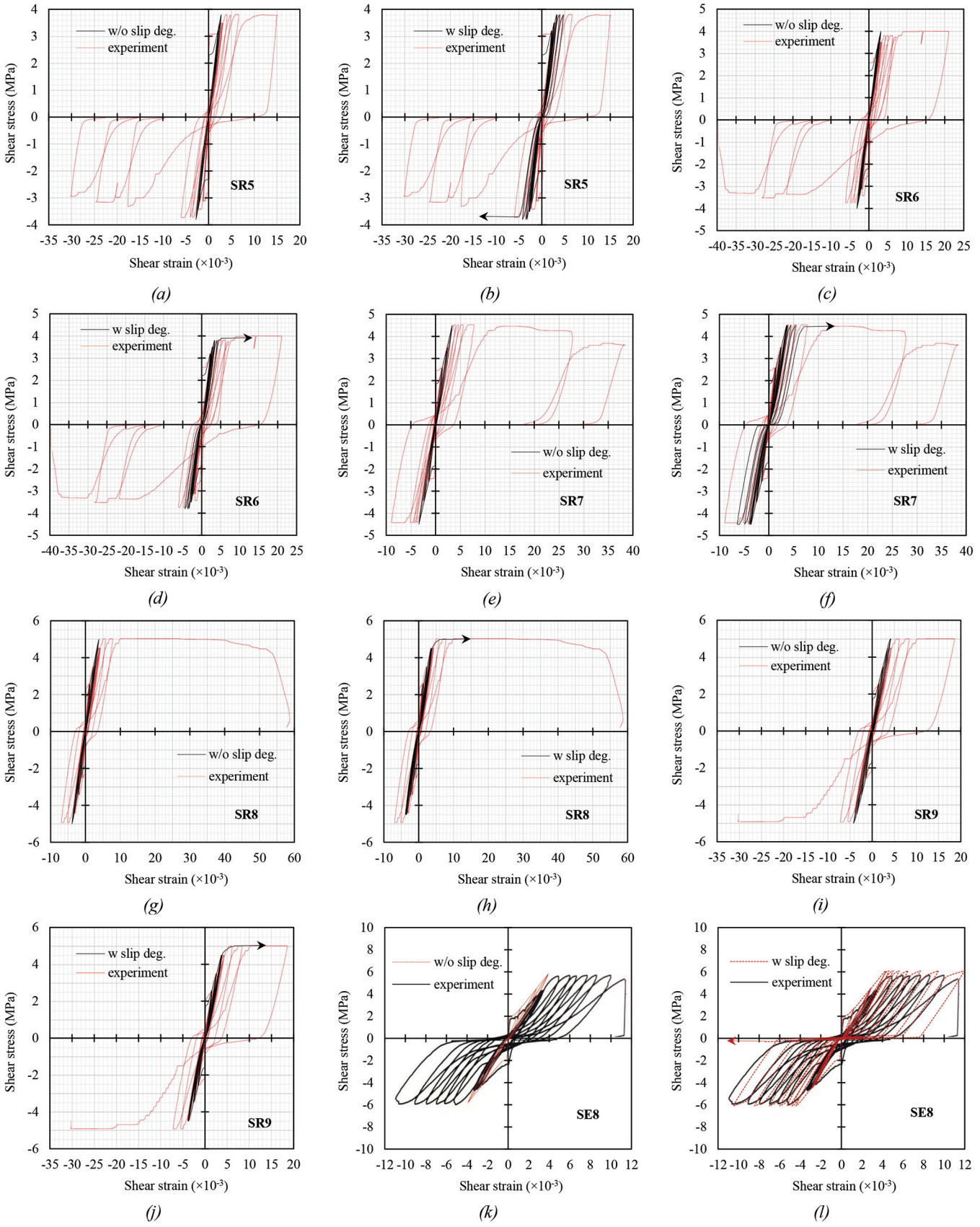

Fig. 7—Shell elements measured versus calculated behavior. (Note: 1 MPa = 0.145 ksi.)

Figure 10 shows the calculated versus observed crack patterns for all the shear wall specimens. A good correlation can be seen between the FEA results and the experimental behavior. There was no significant effect on the crack pattern due to the proposed crack-slip model.

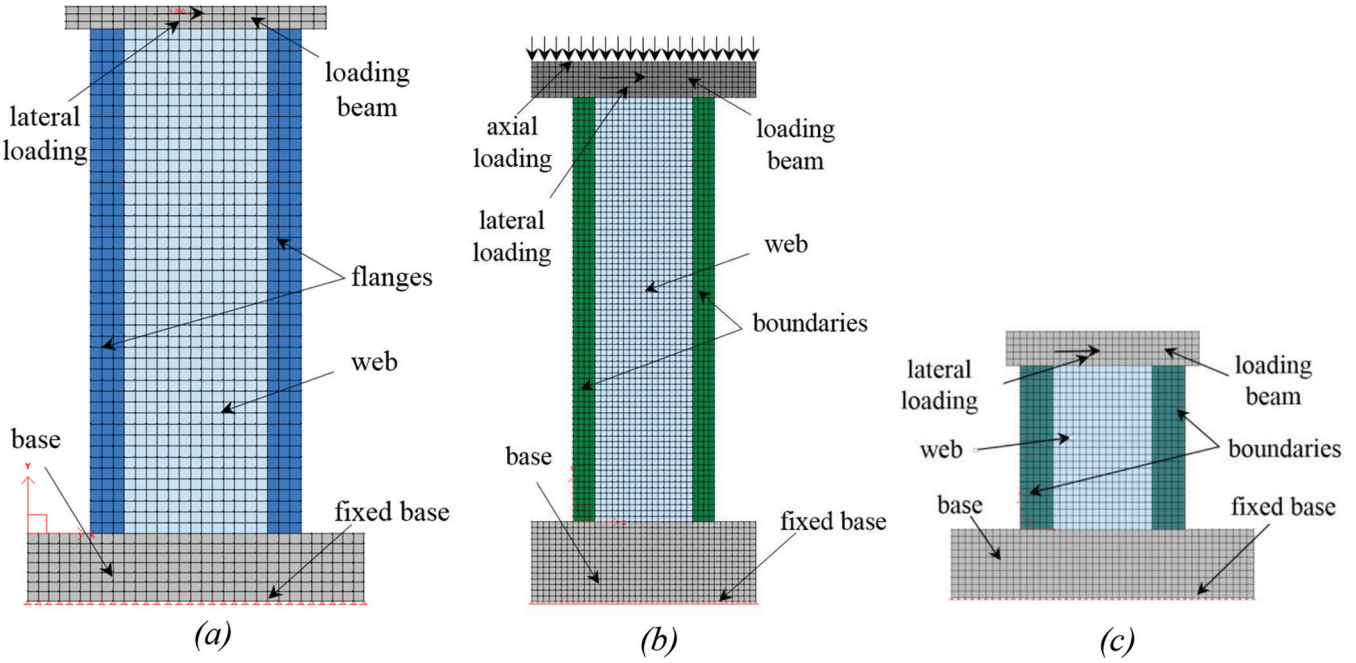

Fig. 8—FE models of shear wall specimens: (a) Wall B2; (b) Wall RW1; and (c) Walls LSW1 and LSW2.

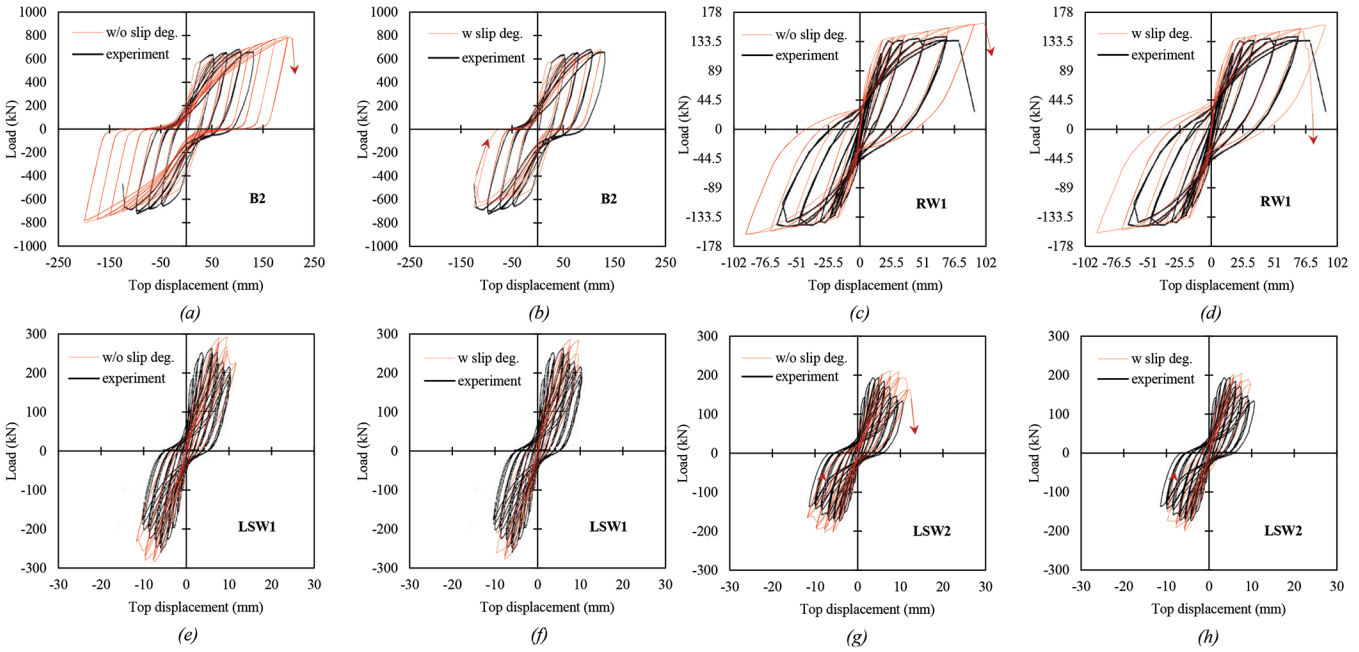

Fig. 9—Shear walls measured versus calculated behavior. (Note: 1 kN = 0.2248 kip; 1 mm = 0.0394 in.)

CONCLUSIONS

The crack-slip model presented herein is an extension of the formulation previously adapted for the DSFM, and includes a crack stiffness degradation law due to cyclic shear stresses on the crack. The degradation factor was empirically derived from cyclic push-off tests. Moreover, a procedure for accounting for a system of two independent rotating cracks within a smeared crack model formulation was described. To verify the proposed methodology, concrete shell elements and shear walls were analyzed. The conclusions that can be drawn from this work are the following:

1. The inclusion of a crack-slip stiffness degradation mechanism, sensitive to the loading history, is necessary for smeared rotating crack models, such as the DSFM, in their application to reversed cyclic loading scenarios.

2. For the proposed model to be a viable phenomenological representation of the crack-slip mechanism, it is required to take into account a minimum of two alternately active, independent rotating cracks.

3. The model verification analyses performed for shell elements yielded imperfect evaluation of the hysteresis loops compared to test observations. Nevertheless, failure was reached analytically by cycling at the same level of stress as during the experiments.

4. The proposed model resulted in good estimates of capacity, ductility, failure mode, and shape of the hysteresis

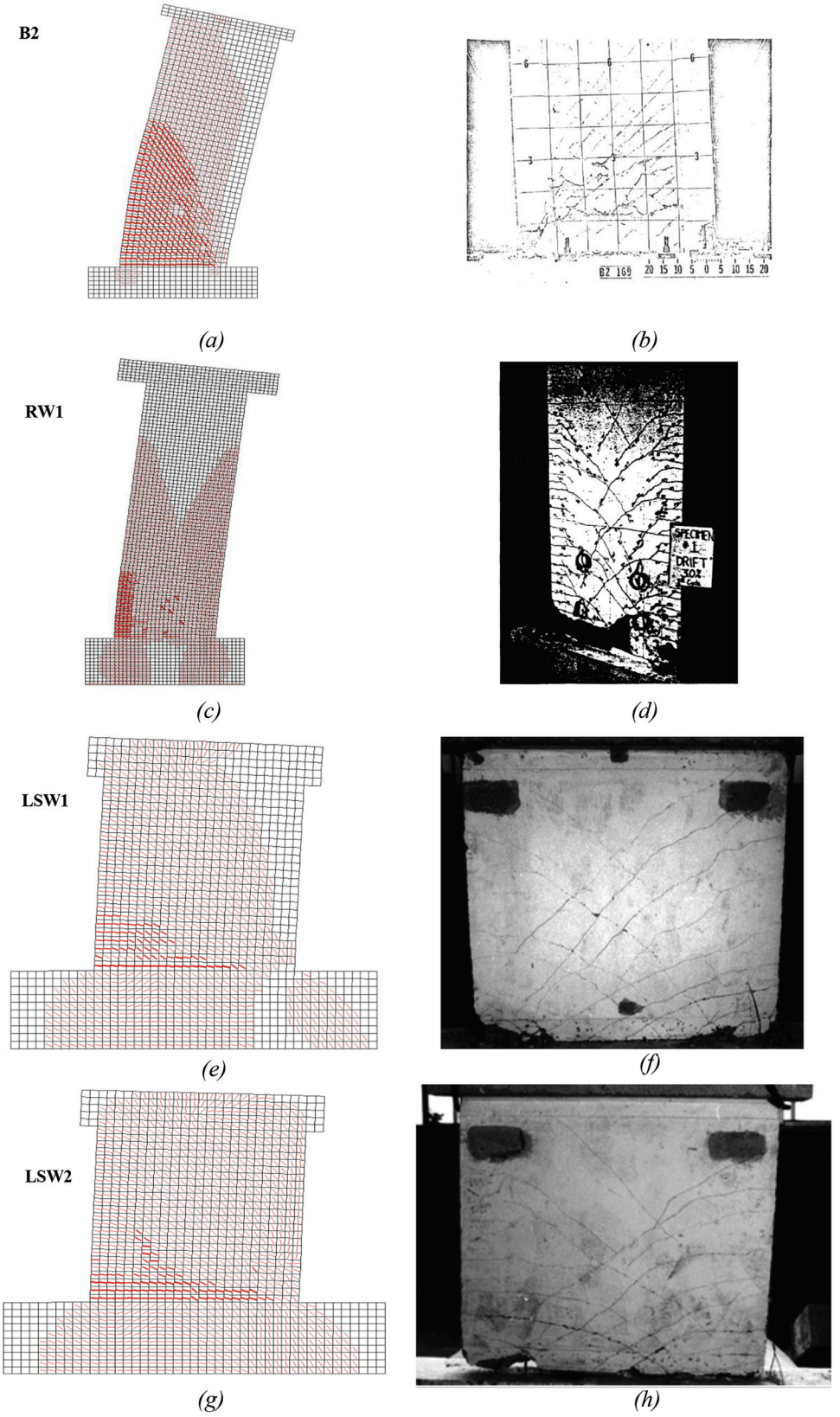

Fig. 10—Shear walls calculated versus observed crack patterns. (Note: 5× amplification factor.)

loops for the shear walls analyzed, compared with the experimentally observed behavior.

5. Compared with the crack-slip model without slip degradation, the proposed model tends to perform better at estimating the behavior of the specimens investigated in this study.

6. The crack spacing calculation was found to influence the crack-slip mode greatly. This was not an unexpected outcome, given the procedure for calculating the slip shear

strains. Nevertheless, special consideration should be given to correctly estimating the crack spacing when using this model.

Additional experimental and analytical work is needed for further improvement. Tests on the cyclic behavior of cracks, investigating parameters such as aggregate size, concrete strength, and variable crack width, could potentially lead to a more accurate degradation law for the crack-slip stiffness, because the number of tests currently available for model calibration is modest.

The procedure can be applied to the analysis and assessment of a large variety of concrete elements. Further studies will include the analysis of elements from the lateral force resisting system of a building, as they are subjected to significant reversed cyclic shear loading during seismic events, greatly contributing to story drifts. Therefore, the behavior of beam-column joints, coupling beams, columns, and shear walls will be investigated with the proposed crack-slip model. The procedure is expected to be particularly useful for cases of high shear demand and for lightly reinforced structures. Analytically, the procedure can be extended to include any direction the rotating crack takes, through a system of more than two independent cracks, and the cyclic degradation law can be enhanced to account for the level of shear stress across the crack. Moreover, the inclusion within the analytical procedure of the compression stresses that develop at the crack interfaces would represent a more accurate representation of the crack-slip mechanism and it could lead to better analytical estimates of the response of concrete elements subjected to cyclic loading. Although the crack-slip model was discussed for two-dimensional application, a similar methodology can be employed for three-dimensional behavior.

AUTHOR BIOS

Anca C. Ferche *is a PhD Candidate in the Department of Civil and Mineral Engineering at the University of Toronto, Toronto, ON, Canada. She received her BASc from Technical University of Cluj-Napoca, Cluj-Napoca, Romania, and her MASc from University of Toronto. Her research interests include performance assessment and analysis of reinforced concrete structures, concrete deterioration mechanisms, and rehabilitation of structures.*

Frank J. Vecchio, *FACI, is a Professor in the Department of Civil and Mineral Engineering at the University of Toronto. He is a member of Joint ACI-ASCE Committees 441, Reinforced Concrete Columns, and 447, Finite Element Analysis of Reinforced Concrete Structures. He is recipient of the following ACI awards: Structural Research Award (1998), Structural Engineering Award (1999), Wason Medal (2011), and Joe Kelley Award (2016). His research interests include advanced constitutive modeling and analysis of reinforced concrete, assessment and rehabilitation of structures, and response to extreme loads.*

REFERENCES

1. Oestrele, R. G.; Fiorato, A. E.; Johal, L. S.; Carpenter, J. E.; and Russell, H. G., "Earthquake-Resistant Structural Walls – Tests of Isolated Walls," *Report* to the National Science Foundation, Construction Technology Laboratories, Portland Cement Association, Skokie, IL, Nov. 1976, 315 pp.

2. Paulay, T.; Priestley, M. J.; and Synge, A. J., "Ductility in Earthquake Resisting Squat Shearwalls," *ACI Journal Proceedings*, V. 79, No. 4, July-Aug. 1982, pp. 257-269.

3. Sittipunt, C., and Wood, S. L., "Influence of Web Reinforcement on the Cyclic Response of Structural Walls," *ACI Structural Journal*, V. 92, No. 6, Nov.-Dec. 1995, pp. 745-756.

4. Thomson IV, J. H., and Wallace, J. W., "Displacement-Based Design of RC Structural Walls: An Experimental Investigation of Walls with Rectangular and T-Shaped Cross Sections," *Report* No. CU/CEE-95/06, Clarkson University, Potsdam, NY, 1995, 373 pp.

5. Vecchio, F. J., "Towards Cyclic Load Modeling of Reinforced Concrete," *ACI Structural Journal*, V. 96, No. 2, Mar.-Apr. 1999, pp. 193-202.

6. Salonikios, T. N.; Kappos, A. J.; Tegos, I. A.; and Penelis, G. G., "Cyclic Load Behavior of Low Slenderness Reinforced Concrete Walls: Design Basis and Test Results," *ACI Structural Journal*, V. 96, No. 4, July-Aug. 1999, pp. 649-661.

7. Palermo, D., and Vecchio, F. J., "Behaviour of Cyclically Loaded Shear Walls," *ASCE Special Publication: Modeling of Inelastic Behavior of RC Structures under Seismic Loads*, 2001, pp. 562-579.

8. Park, R., "A Summary of Results of Simulated Seismic Load Tests on Reinforced Concrete Beam-Column Joints, Beams and Columns with Substandard Reinforcing Details," *Journal of Earthquake Engineering*, V. 6, No. 2, 2002, pp. 147-174. doi: 10.1080/13632460209350413

9. Palermo, D., and Vecchio, F. J., "Compression Field Modeling of Reinforced Concrete Subjected to Reversed Loading: Formulation," *ACI Structural Journal*, V. 100, No. 5, Sept.-Oct. 2003, pp. 616-625.

10. Palermo, D., and Vecchio, F. J., "Compression Field Modeling of Reinforced Concrete Subjected to Reversed Loading: Verification," *ACI Structural Journal*, V. 101, No. 2, Mar.-Apr. 2004, pp. 155-164.

11. Dhakal, R. D.; Pan, T.; Irawan, P.; Tsai, K.; Lin, K.; and Chen, C., "Experimental Study on the Dynamic Response of Gravity-Load Designed Reinforced Concrete Connections," *Engineering Structures*, V. 27, No. 1, 2005, pp. 75-87. doi: 10.1016/j.engstruct.2004.09.004

12. Sagbas, G.; Vecchio, F. J.; and Christopoulos, C., "Computational Modeling of the Seismic Performance of Beam-Column Subassemblies," *Journal of Earthquake Engineering*, V. 15, No. 4, 2011, pp. 640-663. doi: 10.1080/13632469.2010.508963

13. Kolozvari, K.; Orakcal, K.; and Wallace, J. W., "Modeling of Cyclic Shear-Flexure Interaction in Reinforced Concrete Structural Walls. I: Theory," *Journal of Structural Engineering*, ASCE, V. 141, No. 5, 2015. doi: 10.1061/(ASCE)ST.1943-541X.0001059

14. Wong, P. S.; Vecchio, F. J.; and Trommels, H., "VecTor2 and FormWorks User's Manual," *Technical Report*, Dept. of Civil Engineering, University of Toronto, Toronto, ON, Canada, 2013, 318 pp.

15. Saatci, S., and Vecchio, F. J., "Nonlinear Finite Element Modeling of Reinforced Concrete Structures under Impact Loads," *ACI Structural Journal*, V. 106, No. 5, Sept.-Oct. 2009, pp. 717-725.

16. Kim, S. W., and Vecchio, F. J., "Modeling of Shear-Critical Reinforced Concrete Structures Repaired with Fiber-Reinforced Polymer Composites," *Journal of Structural Engineering*, ASCE, V. 134, No. 8, 2008, pp. 1288-1299. doi: 10.1061/(ASCE)0733-9445(2008)134:8(1288)

17. Vecchio, F. J., "Disturbed Stress Field Model for Reinforced Concrete: Formulation," *Journal of Structural Engineering*, ASCE, V. 126, No. 9, 2000, pp. 1070-1077. doi: 10.1061/(ASCE)0733-9445(2000)126:9(1070)

18. Vecchio, F. J., and Collins, M. P., "The Modified Compression Field Theory for Reinforced Concrete Elements Subjected to Shear," *ACI Journal Proceedings*, V. 83, No. 2, Mar.-Apr. 1986, pp. 219-231.

19. Trost, B., "Interaction of Sliding, Shear and Flexure in the Seismic Response of Squat Reinforced Concrete Shear Walls," PhD dissertation, ETH Zurich, Zurich, Switzerland, 2015, 175 pp.

20. Calvi, P. M.; Bentz, E. C.; and Collins, M. P., "Reversed Cyclic Experiments on Shear Stress Transfer across Cracks in Reinforced Concrete Elements," *ACI Structural Journal*, V. 113, No. 4, July-Aug. 2016, pp. 851-859. doi: 10.14359/51688926

21. Stevens, J. N., "Analytical Modelling of Reinforced Concrete Subjected to Monotonic and Reversed Loadings," PhD dissertation, University of Toronto, Toronto, ON, Canada, 1987, 201 pp.

22. Ohmori, N.; Takahashi, T.; Tsubota, H.; Inoue, N.; Kurihara, K.; and Watanabe, S., "Experimental Studies on Nonlinear Behavior of Reinforced Concrete Panels Subjected to Cyclic In-Plane Shear," *Journal of Structural and Construction Engineering*, V. 403, No. 0, 1989, pp. 105-118. doi: (in Japanese)10.3130/aijsx.403.0_105

23. Villani, R. D., "Reinforced Concrete Subjected to Cyclic Loads: A Pilot Study," BASc thesis, University of Toronto, Toronto, ON, Canada, 1995, 147 pp.

24. Mansour, M., and Hsu, T., "Behavior of Reinforced Concrete Elements under Cyclic Shear. I: Experiments," *Journal of Structural Engineering*, ASCE, V. 131, No. 1, 2005, pp. 44-53. doi: 10.1061/(ASCE)0733-9445(2005)131:1(44)

25. Ruggiero, D. M. V., "The Behaviour of Reinforced Concrete Subjected to Reversed Cyclic Loads," PhD dissertation, University of Toronto, Toronto, ON, Canada, 2015, 433 pp.

26. Paulay, T., and Loeber, P. J., "Shear Transfer by Aggregate Interlock," *Shear in Reinforced Concrete*, SP-42, American Concrete Institute, Farmington Hills, MI, 1974, pp. 1-15.

27. Briseghella, L., and Gori, R., "Aggregate Interlock Cyclic Response of R. C. Critical Section," *Proceedings, 8th World Conf. on Earthquake Engineering*, 1984, San Francisco, CA, pp. 501-508.

28. Sagaseta, J., and Vollum, R. L., "Influence of Aggregate Fracture on Shear Transfer Through Cracks in Reinforced Concrete," *Magazine of Reinforced Concrete Research*, V. 63, No. 2, 2011, pp. 119-137. doi: 10.1680/macr.9.00191

29. Walraven, J. C., and Reinhardt, H. W., "Theory and Experiments on the Mechanical Behaviour of Cracks in Plain and Reinforced Concrete Subjected to Shear Loading," *HERON*, V. 26, No 1A, 1981, 68 pp.

30. Tassios, T. P., and Vintzeleou, E. N., "Concrete-to-Concrete Friction," *Journal of Structural Engineering*, ASCE, V. 113, No. 4, 1987, pp. 832-849. doi: 10.1061/(ASCE)0733-9445(1987)113:4(832)

31. Li, B.; Maekawa, K.; and Okamura, H., "Contact Density Model for Stress Transfer Across Cracks in Concrete," *Journal of the Faculty of Engineering*, V. 40, No. 1, 1989, pp. 9-52.

32. Walraven, J. C., "Fundamental Analysis of Aggregate Interlock," *Journal of Structural Engineering*, ASCE, V. 107, No. 11, 1981, pp. 2245-2270.

33. Bažant, Z. P., and Gambarova, P., "Rough Cracks in Reinforced Concrete," *Journal of the Structural Division*, ASCE, V. 106, No. 4, 1979, pp. 819-842.

34. Dabbagh, H., and Foster, S. J., "A Smeared-Fixed Crack Model for FE Analysis of RC Membranes Incorporating Aggregate Interlock," *Advances in Structural Engineering*, V. 9, No. 1, 2006, pp. 91-102. doi: 10.1260/136943306776232927

35. He, X. G., and Kwan, A. K. H., "Modeling Dowel Action of Reinforcement Bars for Finite Element Analysis of Concrete Structures," *Computers & Structures*, V. 79, No. 6, 2001, pp. 595-604. doi: 10.1016/S0045-7949(00)00158-9

36. CEB-FIP, "Model Code for Concrete Structures," Comitè Euro-International du Béton–Federation Internationale de la Precontrainte, Paris, France, 1978, 336 pp.

37. Vecchio, F. J., and Collins, M. P., "The Response of Reinforced Concrete to In-Plane Shear and Nominal Stresses," *Technical Report*, Department of Civil Engineering, University of Toronto, Toronto, ON, Canada, 1982, 332 pp.